Electrochemical Performance of Ni20Cr Coatings Applied by Combustion Powder Spray in ZnCl 2 -KCl Molten Salts

Article *in* International Journal of Electrochemical Science · February 2012

CITATIONS
51

READS
263

6 authors, including:

Jesus Porcayo-Calderon
Universidad de Sonora (Unison)
175 PUBLICATIONS **1,302** CITATIONS
SEE PROFILE

O. Sotelo-Mazon
Universidad Nacional Autónoma de México
18 PUBLICATIONS **236** CITATIONS
SEE PROFILE

V. M. Salinas-Bravo
Instituto Nacional de Electricidad y Energias Limpias
75 PUBLICATIONS **992** CITATIONS
SEE PROFILE

Cinthya Dinorah Arrieta-Gonzalez
Instituto Tecnológico de Zacatepec
19 PUBLICATIONS **114** CITATIONS
SEE PROFILE

Int. J. Electrochem. Sci., 7 **(2012)** 1134 - 1148

International Journal of
ELECTROCHEMICAL
SCIENCE
www.electrochemsci.org

Electrochemical Performance of Ni20Cr Coatings Applied by Combustion Powder Spray in $ZnCl_2$-KCl Molten Salts

J. Porcayo-Calderon[1,*], *O. Sotelo-Mazon*[2], *V.M. Salinas-Bravo*[1], *C.D. Arrieta-Gonzalez*[3], *J.J. Ramos-Hernandez*[4], *C. Cuevas-Arteaga*[2]

[1] Instituto de Investigaciones Eléctricas, Gerencia de Materiales y Procesos Químicos, Reforma 113, Colonia Palmira, C.P. 62490, Cuernavaca, Morelos, MEXICO.
[2] CIICAP-UAEM, Av. Universidad 1001, Col. Chamilpa, C.P. 62209, Cuernavaca, Morelos, MEXICO.
[3] Instituto Tecnológico de Zacatepec, Departamento de Ingeniería Química y Bioquímica, Av. Instituto Tecnológico 27, Zacatepec, Morelos, MEXICO.
[4] Facultad de Química-UNAM, Circuito Exterior S/N, Cd. Universitaria, C.P. 04510, México, D.F., MEXICO.
[*]E-mail: jporcayo@iie.org.mx

Received: 2 December 2011 / *Accepted:* 16 January 2012 / *Published:* 1 February 2012

An investigation about the corrosion resistance of Ni20Cr coatings in $ZnCl_2$-KCl molten salts was carried out by electrochemical techniques. Experimental conditions included static air and temperatures of 350, 400 and 450°C. 304 type SS was evaluated in the same conditions as the Ni20Cr coatings and was used as a reference material to assess the coatings corrosion resistance. Coatings were evaluated as deposited and with a grinded surface finished condition. Electrochemical techniques employed were potentiodynamic polarization curves, open circuit potential measurements and linear polarization resistance curves. Results showed that Ni20Cr coatings have a better performance than 304 type SS due to its high Ni content. The low corrosion resistance of 304 stainless steel was attributed to the low stability of Fe and Cr and their oxides in the corrosive media used. A thermochemical analysis of the Fe-Cr-Ni-Cl-O system is presented to support the results shown.

Keywords: coatings, molten salts, chlorides, thermal spray, thermochemical analysis

1. INTRODUCTION

Molten salt corrosion is a major cause of downtimes and shutdown in the operations of waste incinerators facilities and this represents a large percentage of total maintenance costs of the facility. This is mainly because the fuel material used contains significant amounts of alkali metals (sodium and potassium), heavy metals (lead, tin and zinc) and chloride-containing compounds, which during the combustion process develop into highly corrosive compounds [1].

When a molten salt is present, the salt wets the oxide surface and is able to penetrate through the porous and cracks by capillary action. Transport by diffusion through the molten salt is much faster than solid state diffusion. Therefore, the superficial layer will grow much faster and the important chemical reactions will be those involving the phases present in the molten salt. The molten salts provide a means for the transport of both the oxidant to the metal and dissolved metal ions to the outside. The molten salts are able to permeate through the porosity of the oxide layer and a wide range of local activities of oxygen from oxidizing to reducing conditions can be found. The reactions that form metallic chlorides near the metal-oxide interface will consume the alloy components responsible for repairing the protective oxide scale. Metallic chlorides, which can be formed above or below the oxide-metal interface, can migrate to the melt-gas interface as dissolved species. Because of their porous nature, they can reprecipitate as non-protective oxides providing a route for the continuous penetration of salt and gaseous species [2].

Better understanding of mechanisms of material degradation by salt compounds is an important issue to reduce tube consumption rate in waste incinerators. Coatings are an alternative to manage the corrosion of tube materials. This approach is a feasible alternative to increase the service life of materials [3]. This investigation shows the results of the evaluation of Ni20Cr coatings deposited by combustion powder spray process in a $ZnCl_2$-KCl eutectic mixture.

2. EXPERIMENTAL PROCEDURE

2.1. Coating Procedure

A Ni20Cr (% wt.) powder alloy was used as coating material. Coatings were applied on 0.25 inches diameter AISI 304-type stainless steel rods (304SS) by combustion powder spray (CPS) using a Sultzer-Metco model 5PII system with oxyacetylene flame. In all cases, the same working conditions such as distance of spraying, pressure and flow of gases was maintained for all coatings. Before coating, all rods were cleaned with acetone and their surface was shot blasted with alumina particles according to NACE No.1/SSPC-SP 5 recommended practice [4]. After shot blasting, specimens were cleaned again with acetone and were ready for coating.

2.2. Electrochemical Tests

Corrosion tests were carried out using two surface conditions: as deposited and grinded with 600 grade emery paper.

For electrical connection, specimens were spot welded to a Ni20Cr wire. Ceramic tubes were used for isolating the electrical wire from the molten salt, the gap between the ceramic tube and electrical connection wire was filled with refractory cement. Size, preparation of specimens and corrosive mixtures were the same for electrochemical tests. The corrosion mixture (KCl-$ZnCl_2$) was prepared with analytical grade reagents. Dried chloride salts were first weighted in desired 1:1 mole ratio then subjected to a mechanical milling in an agate mortar to obtain well-mixed reagents. Test

temperatures were 300, 350 and 400°C. A 20 ml alumina crucible was used for containing the corrosive mixture and placed inside an electrical furnace. When the test temperature was stabilized, the three electrochemical cell electrodes were introduced inside the molten salt. In all experiments, the atmosphere above the melt was static air.

For each measurement carried out, the corrosion potential (*Ecorr*), the linear polarization resistance (LPR), and the polarization curves (*Ecorr vs. Icorr*) were obtained. To determine RPL, a potential polarization of ±10 mV was applied and the variation in current intensity associated with that polarization was measured hourly up to a total of 48 hr. Tafel slopes (βa, βb) were obtained from the active regions of the corresponding anodic and cathodic curves by scanning the potential from -400 to 1500 mV applying a scanning rate of 1 mV/s.

Electrochemical tests were carried out using an ACM Instruments Auto DC potentiostat, controlled by a personal computer.

2.3. Specimens Analysis

After testing, corroded specimens were mounted in thermosetting resin and examined in a scanning electronic microscope (SEM) with X-ray energy dispersive (EDX) analyzer.

3. RESULTS AND DISCUSSION

3.1. Coating Features

Figure 1 shows different aspects of the coatings tested. Figure 1(a) correspond to the as deposited superficial condition. It is observed an irregular surface, particles completely deformed (flakes), porosity and partially molten particles.

Coatings in its as deposited condition have an oxidized surface layer formed during the spraying process. In this condition, due the surface roughness is difficult to establish the actual area of reaction and this can affect measurements.

Therefore, in order to homogenize the surface and remove the top oxidized layer all coatings were evaluated in the grinded surface condition, figure 1 (b). In this case there is a homogeneous surface with the presence of porosity and dark phases corresponding to chromium oxides trapped during the projection process.

Figure 1(c) shows the cross section of coatings which also shows the presence of isolated porosity, dark phases, particles in form of flakes parallel to the substrate surface, and particles not deformed. All these characteristics are typical of the coatings deposited by the combustion powder spray process [5]. In order to avoid the presence of galvanic corrosion by the diffusion of molten salts to the substrate coating thickness deposited were at least 500 microns.

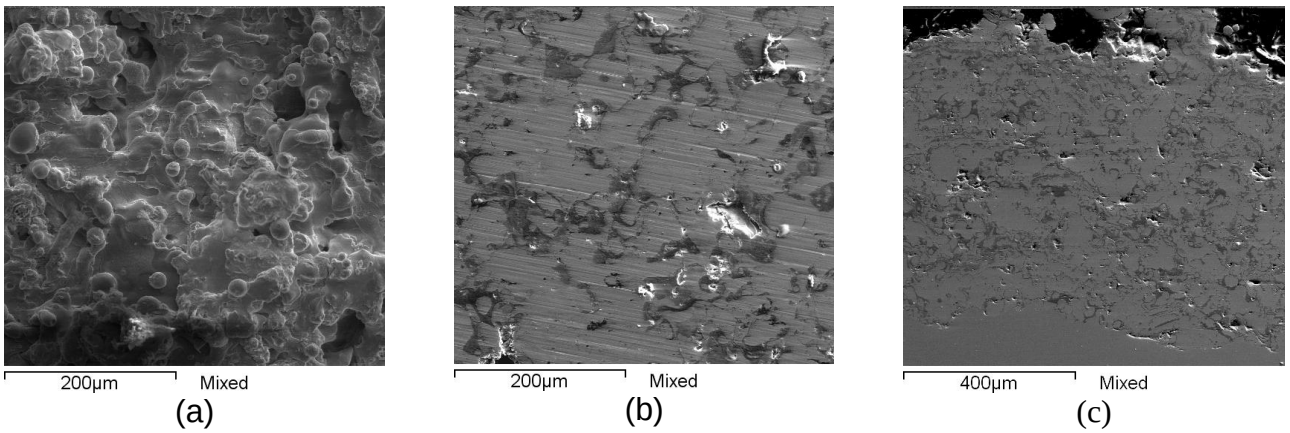

Figure 1. SEM micrographs showing characteristics of the coatings; (a) as deposited surface, (b) grinded surface, and (c) transverse condition.

3.2. Potentiodynamic Polarization Tests

Figures 2 and 3 show the potentiodynamic polarization curves of materials evaluated in $ZnCl_2$-KCl at different test temperatures.

304 SS at 350°C showed the more cathodic *Ecorr* (-202 mV) and the lowest *Icorr* (0.39 mA/cm^2), at 400°C and 450°C *Icorr* values were 2.03 and 1.89 mA/cm^2 respectively. At 350°C, the anodic region of the curve shows a wide passive zone due to the growth of a protective oxide layer on its surface, at 400°C the passive zone is shorter and far from their *Ecorr* potential (600 mV); contrary, at 450°C the alloy was not able to develop a stable protective oxide layer.

Ni20Cr coatings as-deposited at 350°C show more cathodic *Ecorr* (-520 mV) at 400°C and 450°C the *Ecorr* is noblest (-120 mV and -35 mV, respectively). Branches of the anodic polarization curves show the presence of a passive zone at all test temperatures in the range of 100-550 mV at 350°C, 500-1000 mV at 400°C and 340-800 mV at 450°C. The range of the passive zones is similar in all cases: 450-500 mV. This may be due to the presence of the typical oxidized layer of the as-deposited coatings. *Icorr* values are have the same order of magnitude at the three temperatures tested, actually these values are smaller if we consider that due to surface roughness it was not possible to calculate the actual reaction area.

In the as grinded condition, both roughness and surface oxidized layer was eliminated and then calculated reaction area is closer to the actual reaction area. In this case the corrosion potential behavior (*Ecorr*) becomes more cathodic with the test temperature, being 79, -98 and -577 mV at 350°C, 400°C and 450°C, respectively. The anodic branches show that at 350°C, the coating showed a tendency to establish a passive zone between 500 and 1250 mV, at 400°C achieved passivation in the range of 190 to 850 mV, and at 450°C the passive zone is between -100 and 600 mV. In this case the range of the passive zone is greater than in the case of the as-deposited coatings, having a range between 650-750 mV. This may be due to the uniformity of its surface that reduces the available area for adsorption of ionic species. *Icorr* values are similar and have the same order of magnitude. Table 1 shows the electrochemical parameters determined from polarization curves.

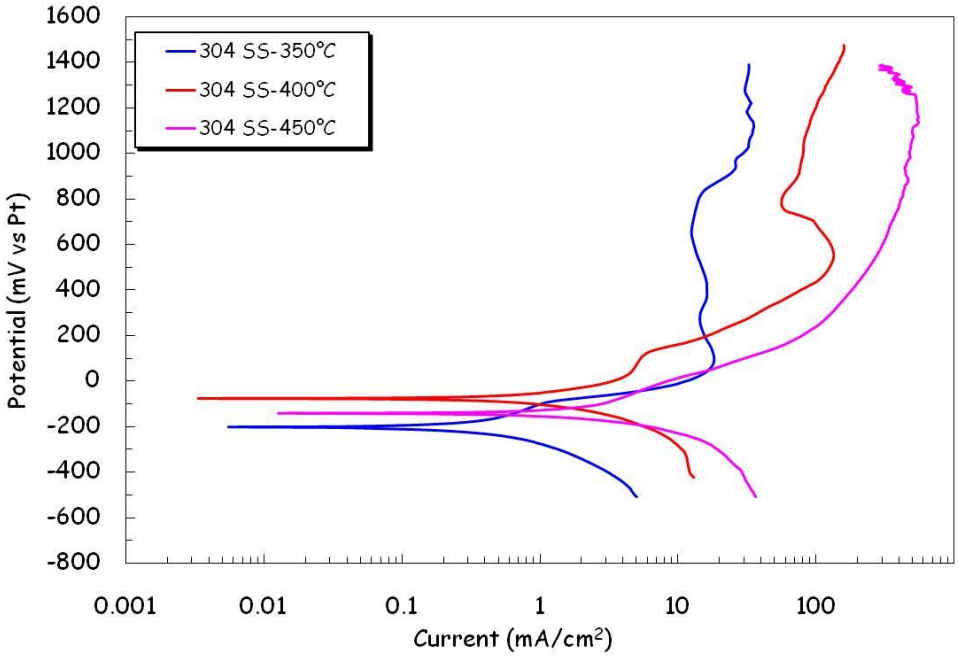

Figure 2. Polarization plots of 304 SS at the different temperatures.

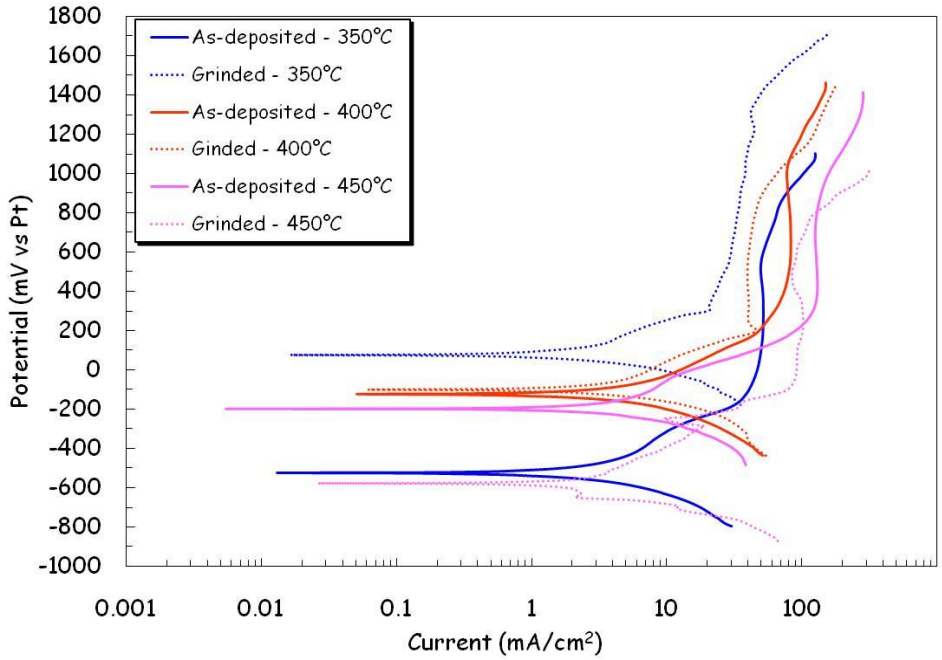

Figure 3. Polarization plots of Ni20Cr coatings at the different temperatures.

According to Table 1 stainless steel had the greater corrosion resistant. However, it should be noted that this behavior correspond to the beginning of the corrosion process. This trend may change in long-term exposures because either the corrosion process can induce changes in the chemistry of the

molten salts, making them more aggressive or the material may not be able to regenerate protective oxide layers.

Table 1. Electrochemical parameters of potentiodynamic polarization tests.

Materials		*Ecorr* (mV)	βa	βc	*Icorr* (mA/cm^2)
304 SS	350°C	-202	137	174	0.39
	400°C	-77	300	277	2.03
	450°C	-141	188	118	1.89
As-deposited coating	350°C	-520	330	202	2.84
	400°C	-120	330	244	5.52
	450°C	-194	271	153	3.61
Grinded coating	350°C	79	211	125	1.90
	400°C	-98	262	147	3.50
	450°C	-577	419	217	3.91

3.3. Open Circuit Potential Curves

Ecorr as a funtion of time for the differents materials tested in $ZnCl_2$-KCl molten salts is shown in Figure 4.

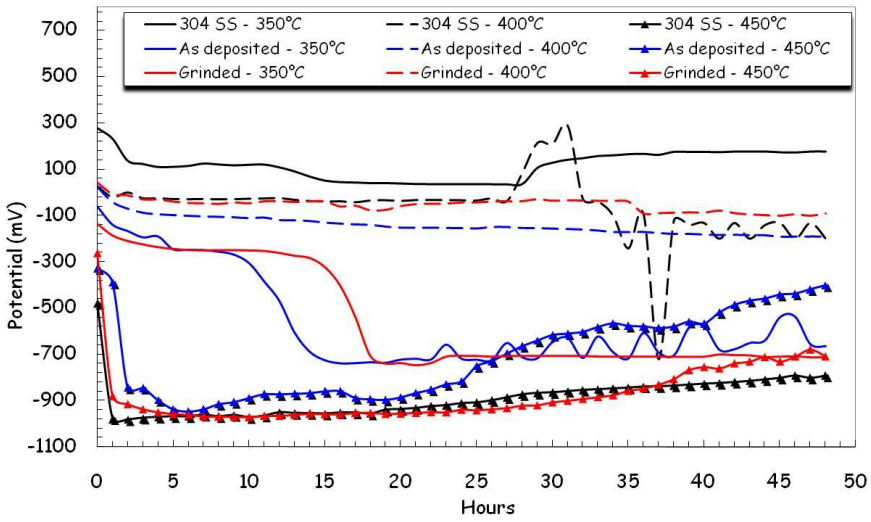

Figure 4. *Ecorr* values as function of testing time for the different materials in $ZnCl_2$-KCl molten salts.

One simple way to study the film formation and passivation of materials immersed in molten salts is by monitoring *Ecorr* as a function of time. A rise of potential in the positive direction indicates formation of a passive film and a steady potential indicates that the film remains intact and protective.

A drop of potential in the negative direction indicates breaks in the film, dissolution of the film, or no film formation. The test temperature significantly affects the *Ecorr* alloys behavior. Usually an increase in temperature increases the aggressiveness of the molten salts and corrosion resistance will depend on the protective capacity of the oxides formed on the alloys.

It is observed that increasing temperature, *Ecorr* values of 304 SS becomes more active. At a temperature of 350°C *Ecorr* decreases up to 28 hours and then tends to increase until the end of the test. This behavior indicates that initially 304 SS experienced a slight corrosion process and subsequently was able to form a protective oxide (Cr_2O_3) that protected it from the action of molten salts. At 400°C *Ecorr* remains almost constant (-25 mV) for 27 hours then shows abrupt changes until the end of the test. This may be associated with the dissolution of protective oxide layers due to the action of molten salts. At 450°C in the first hour of testing, there is a sharp drop of *Ecorr* from -500 mV to -950 mV and then slowly increase to -800 mV until end the test. This indicates a strong attack of the material and a subsequent attempt to form a protective oxide. Another explanation could be the accumulation of corrosion products which prevented the free molten salts access to the corroded surface.

Trend *Ecorr* values for the Ni20Cr coatings either in as-deposited or grinded condition was similar at all temperatures tested. Concerning the Ni20Cr coating as-deposited, at 350°C it is observed that *Ecorr* values decrease during the first 15 hours and then tends to increase showing fluctuations until the end of the test.

The initial behavior can be associated with the dissolution process of the surface oxides and an attempt to selfhealing. At 400°C there is a slight *Ecorr* decrease from 25 mV to -190 mV until the end of the test. At 450°C in the first two hours of test a sharp drop in the *Ecorr* values from -330 mV to -850 mV was observed with a further increase up to -400 mV. This behavior indicates that coating showed a dissolution process of their surface oxides at the beginning of the test and then a passivation process that protected the coating.

In the grinded condition at 350°C it is observed that *Ecorr* values decreases during the first 18 hours and then remains constant around -710 mV. At 400°C there is a slight *Ecorr* decrease from 60 mV to -90 mV until the end of the test. At 450°C in the first hour of immersion was observed a sharp drop in the *Ecorr* values from -230 mV to -900 mV then an increase was observed until -700 mV until the end of the test.

3.4. Linear Polarization Curves

Figure 5 show the evolution of the *Icorr* obtained by linear polarization measurements over time for different materials tested.

At 350°C, 304 SS showed an almost constant *Icorr* between 0.5-1.0 mA/cm^2. This is consistent with the appearance of the material after the corrosion test as seen in Figure 6a. The material formed on its surface a Cr_2O_3 thin layer which protected it from the aggressive environment.

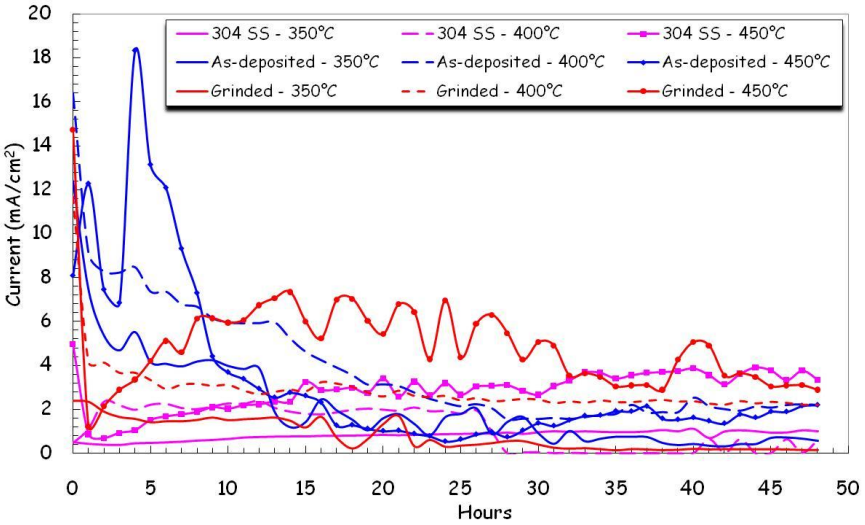

Figure 5. Current density (*Icorr*) plots of different materials evaluated in $ZnCl_2$-KCl molten salts at different temperatures.

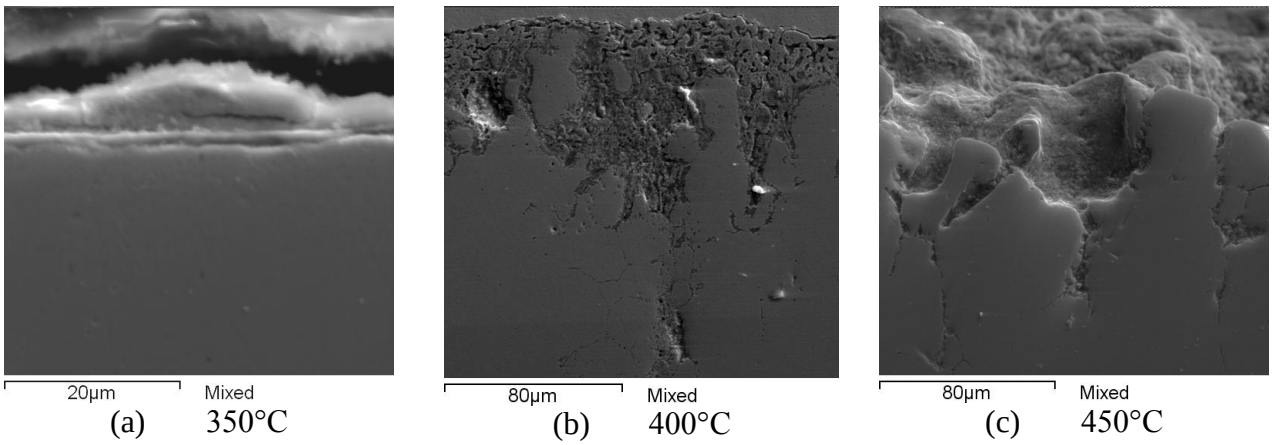

Figure 6. Cross-sectional aspect of the 304 SS after corrosion test in $ZnCl_2$-KCl at different test temperatures.

At 400°C, 304 SS showed an increase in *Icorr* from 0.5 to 2.2 mA/cm^2 in the first two hours of immersion, remaining constant up to 26 hours, and then decrease to very low values until the end of the test. This behavior is not consistent with the material appearance after testing (Figure 6 b). Perhaps initially, the molten salt corroded the material surface and formed a thick layer of corrosion products which prevented penetration of the corrosive agent to the surface and this was manifested as an *Icorr* decrease. However, the internal damage observed indicates that the material degradation was much more severe and this was possibly due to the Cl_2 diffusion which favored its direct reaction with the elements of the alloy. These reactions were solid-gas type, and not taken into account as electrochemical reactions that were obtained by the LPR technique. The external surface of the material shows a sponge-like area with lots of interconnected voids that formed flow channels so the

Cl_2 penetrate into the material; as reported by other authors [2, 6]. Mapping elements to the spongy area (Figure 7) showed an almost total depletion of Cr and Fe, and a Ni enrichment.

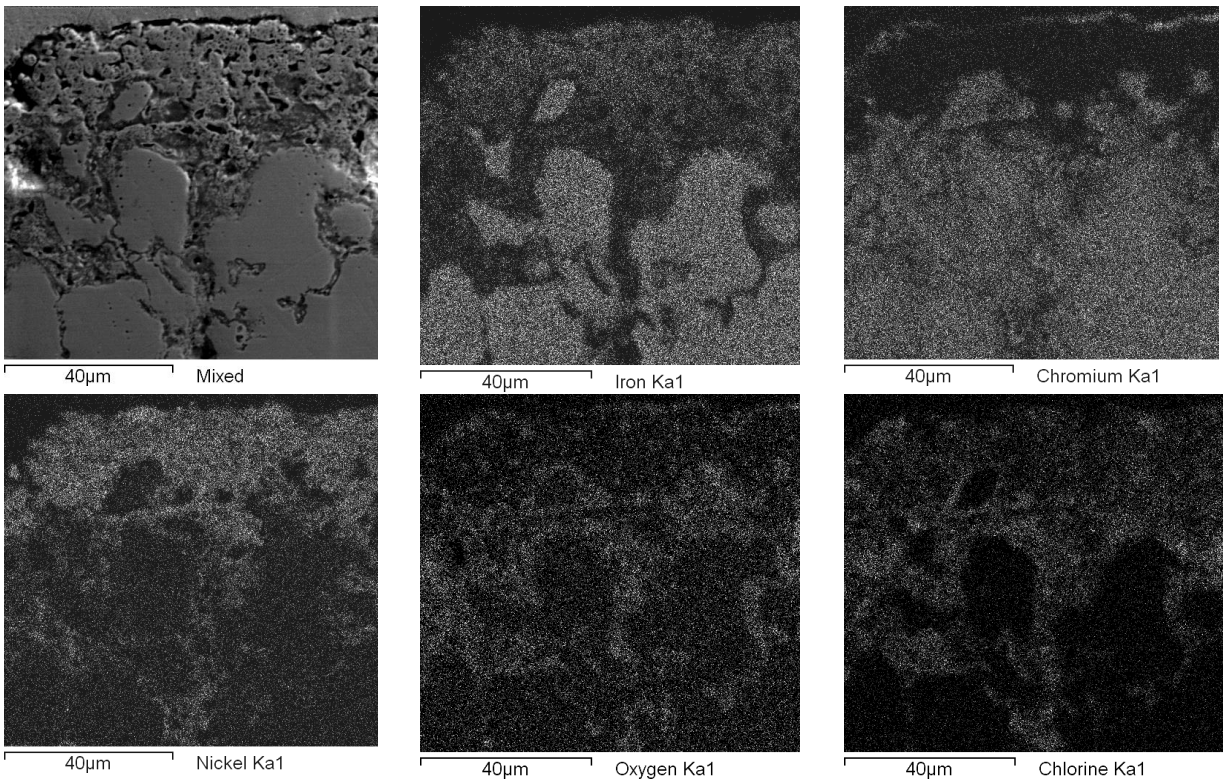

Figure 7. Spongy area of the 304 SS at 400°C and mapping of elements.

Formation of a spongy area suggests that Cl_2 reacted preferably with Cr and Fe oxides to form metallic chlorides in gaseous state which diffuse through the channels and reprecipitated as not protective oxides on the corrosion product scale according to some of the following reactions.

$$Cr_2O_3 + 3Cl_2 = 2CrCl_3 + \frac{3}{2}O_2$$

$$Fe_2O_3 + 2Cl_2 = 2FeCl_2 + \frac{3}{2}O_2$$

$$Fe_3O_4 + 3Cl_2 = 3FeCl_2 + 2O_2$$

These reactions suggest that Fe and Cr oxides are converted into metallic chlorides in environments with low oxygen partial pressure, i.e. this can only occur at the interface metal-molten salt or in the spongy area observed. The metallic chlorides have high vapor pressures and can spread easily through the spongy area to regions with higher oxygen partial pressure where the reverse reaction is favored, i.e. metallic chlorides are oxidized to form not protective metallic oxides. This degradation process by the chloride action has been considered as a process of "active oxidation" which leads to high corrosion rates. During the active oxidation, chloride salts penetrate the porous

layer until sites where their activity increase to promote the reaction of metallic chlorides which dissolve in the salt and spread quickly to the molten salts by transport in gas or liquid phase. At this point, chlorides are oxidized and a release of Cl_2 occurs which returns to repeat the degradation cycle. This mode of transport through the layer is much faster than diffusion in solid state associated with the growth of protective oxide scales in clean environments [6].

At 450°C the 304 SS shows that *Icorr* decreased during the first hour of immersion and then tended to increase steadily to end the test. This behavior shows that initially the material was protected by a protective oxide layer, but this one was not stable because *Icorr* was always increasing. These observations are consistent with the aspect of the 304 SS after corrosion test (Figure 6c). It is noted that the material underwent grain boundary attack and catastrophic corrosion process where molten salts were always in contact with an unprotected surface. According to Li et al. [7], 304 SS in oxidizing environments at 450°C shows intergranular corrosion, in addition, this kind of degradation does not occur in reducing environments [8, 9].

The behavior observed at 400 and 450° C is consistent with other studies [8, 9], which indicates that at the beginning of the corrosion test under deposits of $ZnCl_2$-KCl, the corrosion rates will always be greater due to the presence of Cl^- anions in the eutectic system. This happens because the molten salts dissolve the oxide layer and penetrates it rapidly degrading their protective properties

Concerning Ni20Cr as-deposited coatings, Figure 5 shows that the *Icorr* variation showed the same behavior at 350°C and 400°C, i.e. in both cases *Icorr* tended to decrease throughout the test period. However, at 350°C the *Icorr* was always smaller than at 400°C. At 450°C, a considerable increase in *Icorr* was observed in the first 5 hours, and then tended to decrease to similar values to those observed at 400°C. The highest *Icorr* values observed during the first hours of immersion is due to the dissolution of protective oxides by the corrosive action of molten salts [8]. Figure 8 shows the appearance of coatings as-deposited after the corrosion test. It is observed that at 350°C the coating remained virtually unchanged on its surface, and only shows the presence of corrosive agent on its surface.

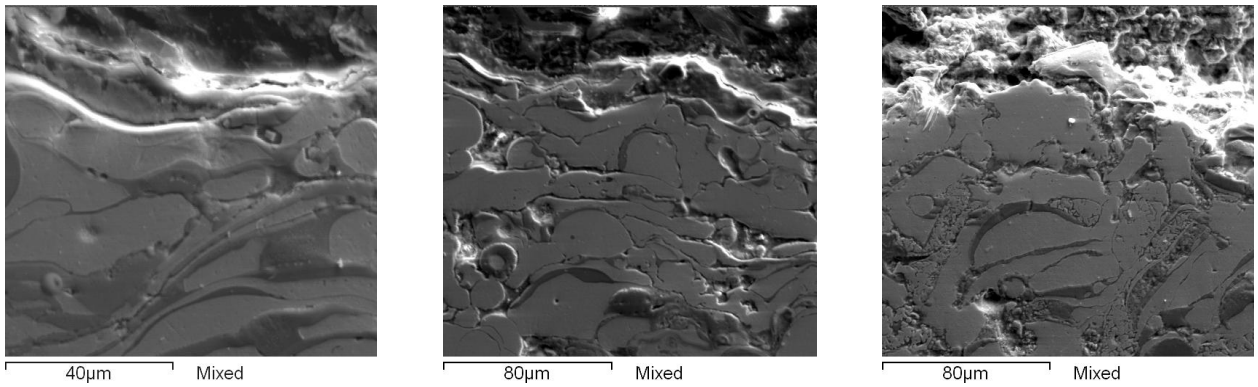

(a) 350°C (b) 400°C (c) 450°C

Figure 8. Cross-sectional aspect of the Ni20Cr as-deposited coatings after corrosion test in $ZnCl_2$-KCl at different test temperatures.

At 400°C molten salts slightly penetrated through the coating surface porosity and no significant degradation is observed. At 450°C is observed a surface deterioration of the coating where the molten salts were able to penetrate deeper into the coating structure and attacked preferentially the dark phases that correspond to the chromium oxides trapped during the thermal spraying process. In all cases the intensity of degradation exhibited by the coatings is smaller than that shown by the 304 SS.Analyzing the Ni20Cr coating in the as grinded surface condition, at 350°C it showed a steady decline in its *Icorr* values from 2 mA/cm^2 to lower values than those shown by 304 SS. This could be due to the growth of a protective oxide layer that prevented the penetration and attack of the molten salts. At 400°C, during the first hour of testing, there is a sharp decrease in *Icorr* values from 11 to 4 mA/cm^2, later showed a steady decline until similar values as those showed by the as-deposited coating (3 mA/cm^2). This indicates that coating had the ability to selfhealing because of the growth on its surface of a protective oxide layer. At 450°C during the first hour of immersion, it was observed a decrease in the *Icorr* values from 15 to 1 mA/cm^2, further on increases to reach a stabilization at the end of the corrosion test (3.5 mA/cm^2). Figure 9 shows the appearance of the as grinded condition coatings after the corrosion test. At 350°C, it is observed that the surface and structure of the coating are virtually intact, at this temperature the coating showed no significant degradation by action of molten salts. At 400°C is observed that the coating surface remains almost intact and only observed a slight penetration of the molten salts through the surface porosity is observed without being degraded. At 450°C it was observed a slight surface degradation of the coating and molten salts penetrated through its porosity which caused the observed increase in *Icorr* values. Coating degradation is smaller than that shown by the 304 SS.

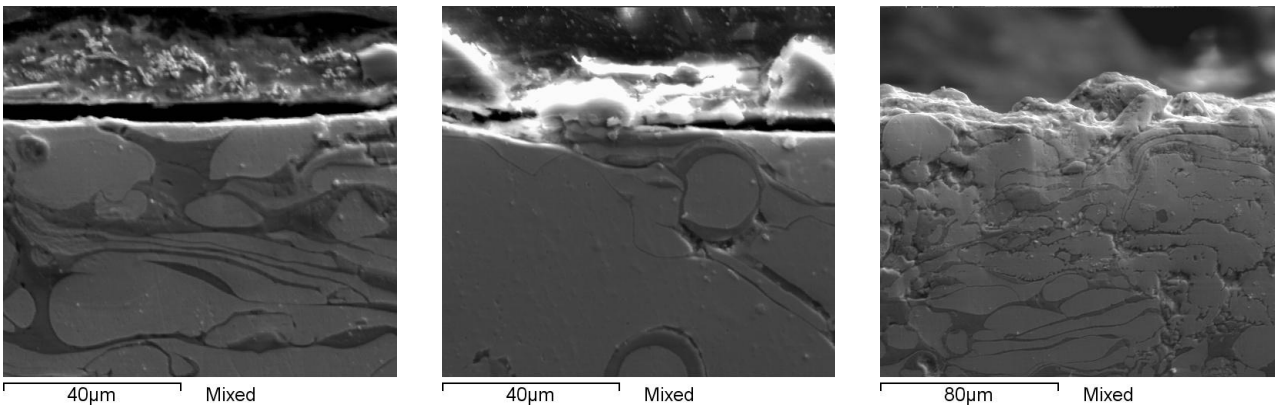

(a) 350°C (b) 400°C (c) 450°C

Figure 9. Cross-sectional aspect of the Ni20Cr grinded coatings after corrosion test in $ZnCl_2$-KCl at different test temperatures.

In both cases it was noted that coatings degradation start to be significant at 450°C. This behavior is because of the preferential attack of molten salts on the chromium oxides trapped into the coating structure during the deposition process. On the other hand, it is known that $NiCl_2$ has a higher thermodynamic stability and a lower vapor pressure compared with iron and chromium chlorides at the

same temperature. On the other hand, the solubility measurements of oxide scales in Cl-rich molten salts showed that NiO is less soluble than the Fe and Cr oxides [10].

The corrosion results described above imply clearly that a high Ni content is very effective in improving the corrosion resistance in a $ZnCl_2$–KCl melt while Cr plays a detrimental role under the same conditions. Is well known that the corrosion protection of any material performing in molten salts depends on the chemical stability of both the metallic elements and their compounds such as oxides and chlorides. This is explained because the breakdown of the protective oxide can occurs by dissolution into the molten salts and the degradation rate can be fast if the oxide has a high solubility.

Considering that Cl_2 and O_2 are the main species of the $ZnCl_2$-KCl-air system that contribute to the degradation of materials in waste incinerators environments, the construction of phase stability diagrams of these species with the main elements of the alloy is a useful tool for understanding the corrosion behavior at high temperature.

Figure 10 shows the phase stability diagrams for the Fe-Cr-Ni-Cl-O system at 350, 400 and 450°C. The procedure to generate the diagrams is described elsewhere [11]. Table 2 shows the set of chemical reactions used for their calculation.

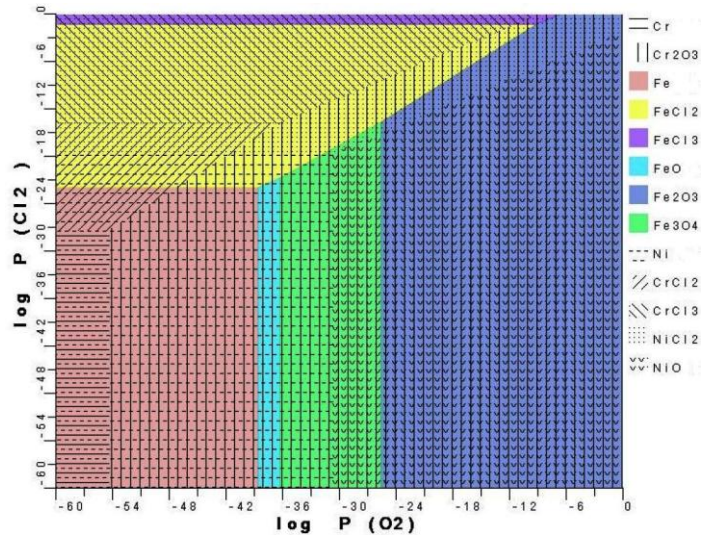

(a)

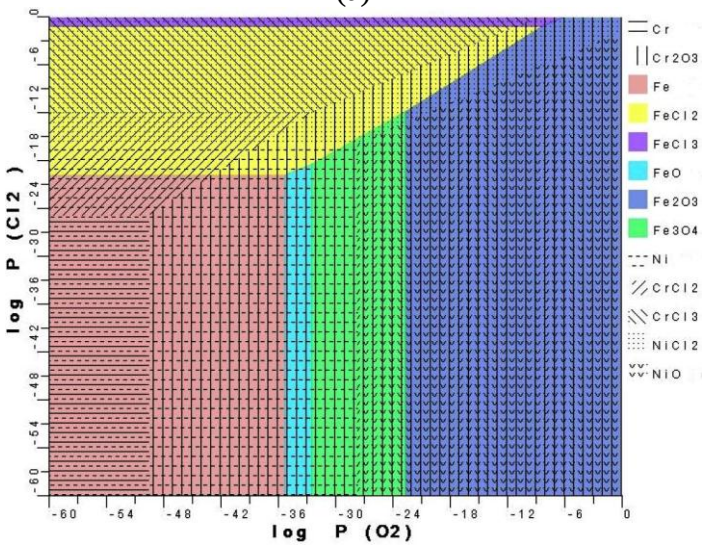

(b)

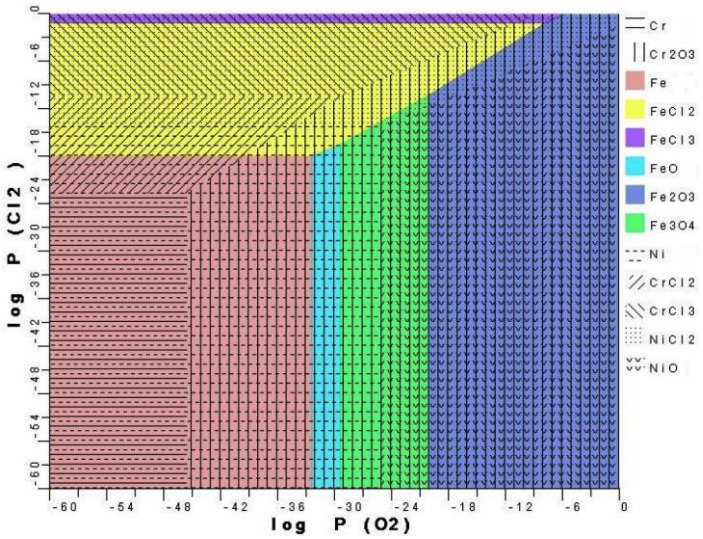

(c)

Figure 10. Thermodynamic stability diagrams for Fe-Cr-Ni-Cl-O at (a) 350°, (b) 400°C and (c) 450°C.

Table 2. Chemical reactions and equilibrium constants for the Fe-Cr-Ni-Cl-O system.

		Log K		
#	Reaction	350°C	400°C	450°C
1	$2Fe + O_2 = 2FeO$	38.5922691425	35.2413475871	32.3567977978
2	$Fe + Cl_2 = FeCl_2$	21.9256207713	19.8321881145	18.0318444645
3	$2FeCl_2 + Cl_2 = 2FeCl_3$	1.3407559401	1.2351122246	1.16095166831
4	$6FeO + O_2 = 2Fe_3O_4$	36.2434475819	32.5350917129	29.3603727101
5	$4Fe_3O_4 + O_2 = 6Fe_2O_3$	25.6158975891	22.6448296298	20.0695952283
6	$2Fe_2O_3 + 4Cl_2 = 4FeCl_2 + 3O_2$	-22.1829861175	-20.3922804013	-18.8496646204
7	$Fe_3O_4 + 3Cl_2 = 3FeCl_2 + 2O_2$	-10.2332651909	-9.63300289352	-9.1198496582
8	$2FeO + 2Cl_2 = 2FeCl_2 + O_2$	5.25897240004	4.42302864196	3.70689113124
9	$2Fe_2O_3 + 6Cl_2 = 4FeCl_3 + 3O_2$	-19.5014742373	-17.9220559521	-16.5277612838
10	$4Cr + 3O_2 = 2Cr_2O_3$	163.012594541	148.888928645	136.727821462
11	$Cr + Cl_2 = CrCl_2$	27.2926155946	24.7926984529	22.6421041752
12	$2CrCl_2 + Cl_2 = 2CrCl_3$	13.7716869051	11.9620337245	10.4048207211
13	$2Cr_2O_3 + 4Cl_2 = 4CrCl_2 + 3O_2$	-53.8421321623	-49.7181348337	-46.1594047607
14	$2Cr_2O_3 + 6Cl_2 = 4CrCl_3 + 3O_2$	-26.298758352	-25.7940673847	-25.3497633185
15	$2Ni + O_2 = 2NiO$	30.6527881243	27.6906715433	25.1404523827
16	$Ni + Cl_2 = NiCl_2$	17.6206500668	15.7412293033	14.1250273922
17	$2NiO + 2Cl_2 = 2NiCl_2 + O_2$	4.58851200924	3.79178706324	3.10960240168

Regarding the metallic elements that compose the 304 SS and the Ni20Cr coatings, it is observed that from the thermodynamic viewpoint Ni is the most stable material. Therefore, Ni will remain immune in O_2 and Cl_2 environments where the Fe and Cr would be corroding continuously.

Therefore, in conditions of environments of garbage incinerators in the rank of 350-450°C temperatures, the Ni-rich alloys and coatings will show better performance compared with those richer in Fe or Cr. This analysis is consistent with reported studies where they indicate that Ni or its alloys show better performance in chlorides-rich environments compared with Fe and Cr or their alloys [12-14]

By contrast, analyzing the oxides that can be formed on 304 SS and Ni20Cr coatings, it is observed that from the thermodynamic point of view, the Cr_2O_3 is the most protective oxide because its stability boundary is located at partial pressures of O_2 lower than that of Ni and Fe oxides. Combining this analysis with the previous observations, it can be assumed that the NiCr-based alloys or coatings will have a better performance than Fe-base alloys. This combined effect has been established in other studies [7-9, 14, 15]

However, according to Li et al. [7], despite that Cr_2O_3 is very stable at very low O_2 partial pressures, the partial pressure of Cl_2 can increase significantly in the oxide-melt interface so that the metallic chlorides can become stable phases instead of the oxides. Moreover, they suggest that because the vapor pressure of chlorides is too high, they diffuse toward the melt-gas interface and they can be reprecipitated as non-protective oxides repeating this cycle to give place to the process defined as "active oxidation". On the other hand, they indicate that the poor adherence of the oxide scale formed on alloys containing Cr may be due to the fact that the chlorides can reprecipitated as Cr_2O_3 at partial pressures much lower than those of Fe and Ni chlorides. In this case, Fe and Ni chlorides require much higher partial pressures of O_2. Considering this mechanism, Cr_2O_3 repricipitates closer to the alloy surface generating more porosity and internal stress.

This kind of analysis is very important in order to determine the different corrosion processes that materials and alloys may experience, however, taking into account the microenvironment created under the molten salts it can modify the actual corrosion reaction pathways.

4. CONCLUSIONS

The better corrosion resistance of Ni20Cr coatings as compared to 304 SS in molten $ZnCl_2$–KCl is related to the high Ni content of the coatings. The corrosion results described imply clearly that a high Ni content of the alloy is very effective in improving the corrosion resistance while Cr plays a detrimental role. The slight degradation experienced by the coatings was due to the preferential attack of the chromium oxides trapped into the coating structure during the deposition process. The higher thermodynamic stability of the Ni chlorides and its lower vapor pressure compared with that of iron and chromium chlorides contributed by one side to the best performance of the coatings, and on the other hand to the catastrophic attack of the 304 stainless steel.

ACKNOWLEDGEMENTS
Financial support from CONSEJO NACIONAL DE CIENCIA Y TECNOLOGIA (Conacyt, Mexico) and Master Science scholarship to O. Sotelo-Mazon is gratefully acknowledged.

References

1. Bart E.M. Adams, Kris K.E. Peters, Herman S.W. Diederen and Jac P.F. Winjhoven. Waste Management World, September-October 2004.
2. David A. Shores, Bani P. Mohanty. *Corr. Sci.* 46 (2004) 2909.
3. Adams B., Peeters K., Earaets D., Diederen H. and Wijnhoven J.P.F., Seghers. "Boiler Prism: A proven primary measure against high temperature corrosion". 12th North American Waste-to-Energy Conference, Savannah Georgia, USA, May 2004
4. Joint Surface Preparation Standard NACE No. 1/SSPC-SP 5. White Metal Blast Cleaning.
5. L. Pawlowski, The Science and Engineering of Thermal Spray Coatings, John Wiley & Sons Ltd, (Second edition) 2008.
6. Bani P. Mohanty, David A. Shores. *Corr. Sci.* 46 (2004) 2893.
7. Y.S. Li, Y. Niu, W.T. Wu. *Materials Science and Engineering* A345 (2003) 64.
8. W.M. Lu, T.J. Pan, K. Zhang, Y. Niu. *Corr. Sci.*, 50 (2008) 1900.
9. T. J. Pan, C. L. Zeng, and Y. Niu. *Oxidation of Metals*, 67, 1/2, (2007) 107.
10. T. Ishitsuka, K. Nose. *Corr. Sci.*, 44 (2002) 247.
11. J.J. Ramos-Hernández, 2009. Análisis termoquímico del sistema V-Na-S-O-M y su aplicación en el proceso de corrosión a alta temperatura. *Universidad Nacional Autónoma de México, Tesis de Maestría.*
12. Andreas Ruh, Michael Spiegel. *Corr. Sci.*, 48 (2006) 679.
13. Y.S. Li, M. Spiegel. *Corr. Sci.*, 46 (2004) 2009.
14. K. Yamada, Y. Tomono, J. Morimoto, Y. Sasaki, A. Ohmori. *Vacuum*, 65 (2002) 533.
15. Y. Kawahara. *Corr. Sci.*, 44 (2002) 223.